

Electroweak Physics at the LHC

PHILIP SOMMER ON BEHALF OF THE ATLAS, CMS AND LHCb COLLABORATIONS

The University of Sheffield

Summary. — With the large integrated luminosities recorded at the LHC and the excellent understanding of the LHC detectors, it is possible to measure electroweak observables to the highest precision. A review of the measurement of the W boson mass by the ATLAS Collaboration as well as a new measurement of the electroweak mixing angle with the CMS detector are presented. Special emphasis is put on a discussion of the modelling uncertainties and the potential of the latest low- μ runs, recorded at the end of 2017 by both collaborations.

In addition, the latest measurements of multi-boson final states as well as the electroweak production of single gauge bosons at 13 TeV are summarised. The study of these processes can be used to constrain anomalous gauge couplings in an effective field theory approach, allowing to bridge tests of the electroweak sector of the Standard Models also to Higgs boson production.

1. – Introduction

The electroweak theory makes precise predictions of the properties of the electroweak gauge bosons W , Z and the photon γ . Their masses and their couplings to fermions and to one another can be expressed in terms of the coupling constant of the $SU(2)_L$ gauge group, g , the coupling constant of the $U(1)_Y$ gauge group, g' , and the vacuum expectation value of the Higgs field, v . Measurements at the ATLAS [1], CMS [2] and LHCb [3] experiments at the LHC [4] put the electroweak theory to stringent experimental tests.

The cross sections of electroweak processes accessible at the LHC span eight orders of magnitude, from several nb for the production of single W and Z bosons to multiboson processes with cross sections as small as 1 fb. Measurements in W and Z boson events already reach a high precision of better than one percent on a fraction of the datasets recorded until today. They are the most demanding in terms of detector performance and the modelling of the underlying process. Measurements in diboson processes are sensitive to the gauge structure of the electroweak theory, reach a precision of better than 10% and meanwhile are limited by systematic uncertainties. Studies of processes involving more than two gauge bosons in the final state or the scattering of electroweak gauge bosons are rendered possible for the first time in the large datasets recorded by the LHC experiments in the years 2015 and 2016. Here, the focus lies on first experimental

confirmations of the respective processes. In the following, the most recent results of measurements in the electroweak sector are presented.

2. – Electroweak precision measurements

The fundamental parameters of the electroweak theory relate the masses of the W and Z bosons, m_W and m_Z , via the electroweak mixing angle, $\sin \theta_W$. The precise knowledge of m_Z and $\sin \theta_W$ hence allows to make a precise prediction of m_W . This prediction is sensitive to the masses of other particles of the Standard Model, in particular the masses of the Higgs boson and the top quark, or beyond through radiative corrections that modify the W boson propagators and vertices.

A measurement of the W boson mass has been performed by the ATLAS experiment using 4.6 fb^{-1} of data taken in 2011 at a centre of mass energy of $\sqrt{s} = 7 \text{ TeV}$ [5]. The W boson mass, m_W , is determined from fits of $W \rightarrow \ell\nu$ events simulated with different mass hypotheses to distributions of the reconstructed lepton transverse momentum, p_T , and the transverse mass of the lepton-neutrino system, m_T . Roughly 14 million $W \rightarrow \ell\nu$ events are available in the dataset. The limited detector resolution and the boost of the W boson in the transverse plane can distort and shift these distributions significantly and hence introduce systematic uncertainties. In order to improve the theoretical description, the simulated samples of $pp \rightarrow W \rightarrow \ell\nu$ events are sequentially reweighted to more sophisticated theoretical calculations and measurements in data. The W boson rapidity spectrum is reweighted to a fixed order calculation at next-to-next-to-leading order [6]. Furthermore, the simulated event samples are reweighted to results of a differential measurement of the $pp \rightarrow Z$ cross section expanded in terms of spherical harmonics [7]. The transverse momentum of the W boson, p_T^W , is obtained from a tune of Pythia8 to the Z boson p_T measured in data [8]. A total of 28 individual measurements of the W boson mass are performed. Final states with electrons and muons and with positive and negative electric charge are used. Values of m_W are measured from the p_T and m_T distributions and in different bins of the lepton pseudo-rapidity, η . The individual measurements are then combined accounting for the experimental and theoretical correlations. Results from fits to the m_T distribution have slightly larger uncertainties than the results using fits to the p_T distribution in particular due to uncertainties related to the measurement of the momentum of particles recoiling against the W boson. Otherwise the individual measurements are comparable in precision.

The mass of the W boson is measured to:

$$(1) \quad m_W = 80370 \pm 7(\text{stat.}) \pm 11(\text{exp. syst.}) \pm 14(\text{mod. syst.}) \text{ MeV}.$$

The measurement is systematically limited. However, there is no individual source of systematic uncertainties which strongly limits the measurement. Large sources of uncertainty include the calibration of electrons and muons, the QCD modelling in the parton shower and uncertainties in the parton distribution functions (PDF). The measurement is in agreement with previous measurements at the Tevatron and LEP. It reaches the same precision as the measurement by the CDF experiment [9] which is the most precise individual measurement of m_W . The measurement is also in very good agreement with the indirect determination of m_W using the theoretical interrelation to m_Z . A comparison of the measurement and the value determined indirectly from the global electroweak fit [10] is shown in Fig. 1. The aforementioned sensitivity to the top-quark mass through radiative corrections is also shown. Studies hint that the CMS collaboration can perform

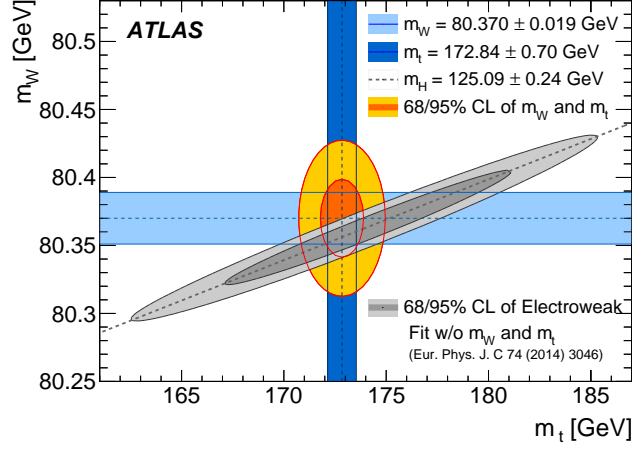


Fig. 1. – Values of the W boson and top quark masses, m_W and m_t , as measured by the ATLAS experiment. The 68% and 95% confidence-level contours are compared to contours determined indirectly from the global electroweak fit [5, 10].

the measurement of m_W with similar precision [11]. Compared to the measurement by the ATLAS experiment a higher relevance of the transverse mass fits is expected since the recoil can be determined more accurately while uncertainties in the lepton calibration are slightly larger.

Future measurements of m_W will rely on a repetition of the detector calibration and the auxiliary measurements used in the reweighting approach. Improvements are needed to cope with the harsher experimental conditions in the data taken at $\sqrt{s} = 13$ TeV due to a higher number of additional inelastic pp interactions in the same bunch-crossing. Methodical improvements could lie in an improved knowledge of p_T^W where the measurement of m_W solely relies on the theoretical extrapolation from p_T^Z . The extrapolation using Pythia8 differs from state-of-the-art calculations using analytic resummation for values of $p_T^{W,Z} < 6$ GeV. An obvious improvement for the measurement of m_W is therefore a direct measurement of p_T^W . To allow for such a direct measurement the LHC was operating with a low number of additional inelastic pp interactions in the same bunch-crossing of $\langle \mu \rangle = 2$ in the end of 2017. This data allows for a precise measurement of the particles recoiling against the W boson to which the measurement of p_T^W is extraordinarily sensitive to. The measurement aims at a precision of 1% for low values of p_T^W [12].

The effective leptonic electroweak mixing angle, $\sin^2 \theta_{\text{eff}}$, was extracted recently, as well, using 19.6 fb^{-1} of pp collisions at a centre of mass energy of $\sqrt{s} = 8$ TeV recorded by the CMS detector [13]. The measurement uses the forward-backward asymmetry, A_{FB} , in $Z \rightarrow \ell\ell$ ($\ell = e, \mu$) events which is sensitive to $\sin^2 \theta_{\text{eff}}$ through the interference of vector and axial-vector neutral currents. The forward-backward asymmetry is defined from the polar angle θ^* in the Collins-Soper-Frame of the dilepton decay system:

$$(2) \quad A_{\text{FB}} = \frac{\sigma(\cos \theta^* > 0) - \sigma(\cos \theta^* < 0)}{\sigma(\cos \theta^* > 0) + \sigma(\cos \theta^* < 0)}.$$

In pp collisions the production of a Z boson can involve a valence and a sea quark or

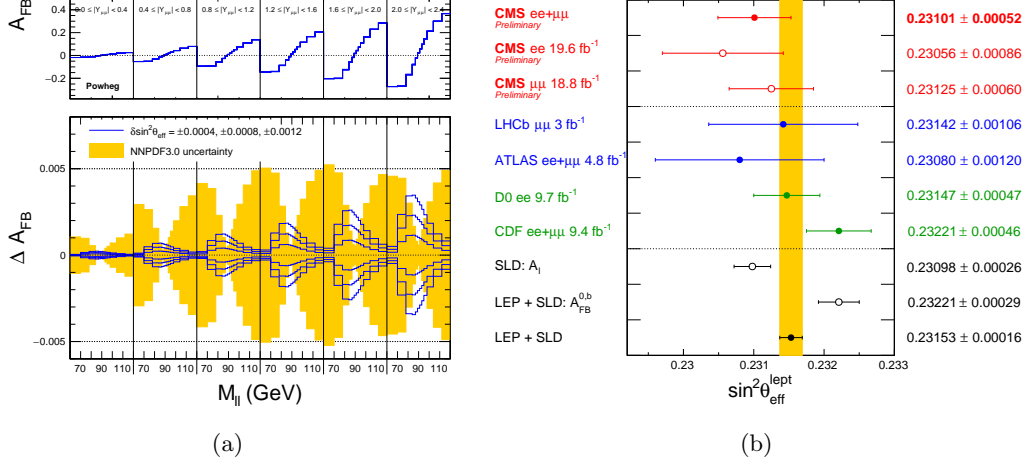


Fig. 2. – (a) The forward-backward asymmetry A_{FB} in bins of the dilepton invariant mass, $m_{\ell\ell}$, and the dilepton rapidity, $|y_{\ell\ell}|$. The upper pad shows the value of A_{FB} in simulated events and the lower pad shows deviations of A_{FB} from the nominal value under variations of $\sin^2 \theta_{\text{eff}}$ and variations of the NNPDF3.0 PDF set within its uncertainty [13]. (b) Comparison of the values of $\sin^2 \theta_{\text{eff}}$ as measured by the LEP, SLD, Tevatron and LHC experiments [13].

two sea quarks. A non-zero forward backward asymmetry is only generated by those interactions that involve valence quarks. The measurement of A_{FB} therefore depends on the knowledge of the direction of the incoming valence quark direction and is diluted by contributions of interactions with two sea quarks. Consequently, the forward-backward asymmetry is most pronounced if the Z boson is boosted in the forward direction, i.e. for high values of the dilepton rapidity, $|y_{\ell\ell}|$. In the CMS experiment the reconstruction of leptons is restricted to a pseudo-rapidity range of $|\eta| < 2.4$ which also restricts the dilepton rapidity to $|y_{\ell\ell}| < 2.4$. The double differential values of A_{FB} in bins of $m_{\ell\ell}$ and $|y_{\ell\ell}|$ are shown in Fig. 2(a). Also shown are the deviations of A_{FB} from the nominal value under variations of $\sin^2 \theta_{\text{eff}}$ and variations of the PDF set within its uncertainty. Both show a different dependence on $m_{\ell\ell}$ and $|y_{\ell\ell}|$. This shape difference allows to constrain the PDF uncertainties in the measurement which effectively reduces the PDF uncertainty from $\pm 0.25\%$ to $\pm 0.13\%$.

The effective electroweak mixing angle is extracted in a fit of the measured forward-backward asymmetry to theoretical predictions based on event samples simulated with different values of $\sin^2 \theta_{\text{eff}}$ to:

$$(3) \quad \sin^2 \theta_{\text{eff}} = 0.23101 \pm 0.00036(\text{stat.}) \pm 0.00018(\text{syst.}) \pm 0.00016(\text{theo.}) \pm 0.00030(\text{pdf}).$$

It is compared to previous measurements in Fig. 2(b). The CMS results is in agreement with the combination of the results of the LEP and SLC experiments [14] which is the most precise value of $\sin^2 \theta_{\text{eff}}$. It reaches a precision comparable to individual measurements by the D0 and CDF collaborations. Both have recently been combined improving the precision by 30% [15]. Of the results from the LHC experiments it is the most precise improving by a factor of two over the measurement by the LHCb collaboration [16]. It

should be noted that the LHCb experiment has the advantage of being able to probe values of the dilepton rapidity to larger values, $2.0 < |y_{\ell\ell}| < 4.5$. While the current LHCb measurement is statistically limited, the larger dataset available in Run 2, along with improved analysis techniques will allow a more precise measurement to be made in the near future. A measurement of A_{FB} was performed by the ATLAS experiment extending to $|y_{\ell\ell}| < 3.6$ [17]. However, no value of $\sin^2 \theta_{\text{eff}}$ was obtained.

3. – Measurements of Diboson Production

The non-Abelian structure of the $\text{SU}(2)_L \times \text{U}(1)_Y$ gauge group causes trilinear and quartic self-interactions between W bosons, Z bosons and photons. The electroweak theory makes precise predictions of these couplings and their strengths. Measurements of the production of two heavy gauge bosons, WW , WZ and ZZ , are sensitive to the trilinear self interactions and have been performed by the ATLAS and CMS experiments at $\sqrt{s} = 7$ TeV, $\sqrt{s} = 8$ TeV and $\sqrt{s} = 13$ TeV, using the datasets recorded in the years 2011, 2012 and 2015, respectively. While previous results saw tensions between data and theoretical calculations at next-to-leading order in the perturbative expansion, the agreement is substantially improved when these calculations are performed at next-to-next-to-leading order. Trilinear self interactions can further be probed in the associated production of a heavy gauge boson with a photon. Quartic self interactions can be studied in the production of three gauge bosons. Such measurements have not yet been performed at $\sqrt{s} = 13$ TeV and are therefore not discussed here.

Recently, the measurements of the $pp \rightarrow ZZ$ production cross section in final states with four leptons have been updated to include 36 fb^{-1} of pp collisions recorded in the years 2015 and 2016 [18, 19]. The measured fiducial cross sections reach an unprecedented precision of $\pm 5.3\%$ and are found in agreement with the theoretical prediction at $\mathcal{O}(\alpha_S^2)$ and corrected for effects of $\mathcal{O}(\alpha_S^3)$ and $\mathcal{O}(\alpha_{\text{EW}}^6)$ for certain subprocesses. For the first time the measurement is systematically limited. The large dataset and the fact that the 4ℓ final state can be fully reconstructed allow for a detailed study of the kinematic properties of $pp \rightarrow ZZ$ production. Differential measurements in a number of kinematic and angular single- and multi-lepton quantities are performed. As an example, the differential measurement of the transverse momentum of the ZZ system by the ATLAS collaboration is shown in Fig. 3(a). This variable is particularly relevant for measurements of $pp \rightarrow WW$ production which typically removes events with hadronic jets. The transverse momentum of the diboson system is directly correlated to that of the jet. As shown in Fig. 3(a), state-of-the-art next-to-leading order event generators which include parton shower programs provide a reasonable description of the p_{T}^{ZZ} spectrum, in particular a better description than fixed order calculations at next-to-next-to-leading order. Furthermore, differential distributions of the properties of hadronic jets accompanying the ZZ production are measured by the ATLAS experiment. Upper limits on neutral trilinear gauge couplings are set in a model independent effective field theory approach using the reconstructed m_{ZZ} (CMS) or p_{T}^Z (ATLAS) distribution. The observed limits improve on previous limits obtained in 20 fb^{-1} of pp collisions at $\sqrt{s} = 8$ TeV by a factor of two. The constraints derived by the CMS collaboration are slightly more stringent than those derived by the ATLAS collaboration.

The analysis by the CMS collaboration adds measurements of the $Z \rightarrow 4\ell$ cross section and branching ratio, and the full $pp \rightarrow ZZ$ line shape in the range $80 \text{ GeV} < m_{\ell\ell} < 1000 \text{ GeV}$. The latter includes contributions from $pp \rightarrow H \rightarrow ZZ^*$ production and is shown in Fig. 3(b).

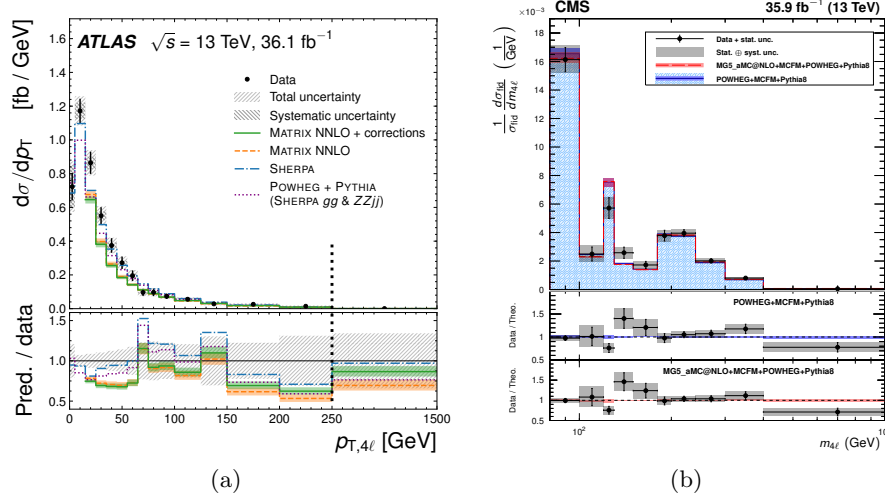


Fig. 3. – (a) Differential fiducial $pp \rightarrow ZZ \rightarrow 4\ell$ cross section as a function of p_T^{ZZ} . The measurement in data is compared to theoretical predictions from state-of-the-art event generators and fixed order calculations [19]. (b) Differential $pp \rightarrow 4\ell$ cross section as a function of $m_{4\ell}$. In addition to the production of two on-shell Z bosons, the measurement is sensitive to $pp \rightarrow Z \rightarrow 4\ell$ and $pp \rightarrow h \rightarrow 4\ell$ production at values of $m_{4\ell} \sim 91$ GeV and $m_{4\ell} \sim 125$ GeV, respectively [18].

4. – Measurements of Vector Boson Fusion and Scattering

An alternative way to study electroweak self interactions in pp collisions is the electroweak production of gauge bosons and two jets. In these cases one or two heavy gauge bosons are produced from two virtual gauge bosons radiated off the partons. The two processes are referred to as vector boson fusion and vector boson scattering, respectively. The latter class of processes involves quartic gauge couplings and is a sensitive probe of electroweak symmetry breaking and the role of the Higgs boson in the renormalisability of the electroweak theory. The specific production mechanism of vector boson fusion and scattering does not involve any flow of colour current and therefore little hadronic activity. It is manifested in the experimental signature of two high p_T jets in the forward region with high invariant mass and large angular separation. The production cross sections for the electroweak production processes are typically a factor of ten smaller than the production cross sections of the same final state via the strong force.

Measurements of electroweak Zjj production have been performed at $\sqrt{s} = 13$ TeV by both the ATLAS and the CMS collaborations [20, 21]. They are based on 3.2 fb^{-1} and 35.9 fb^{-1} , respectively. The characteristic signatures discussed above are used in the selection of candidate events. In the fiducial phase space that differs between both analyses the cross sections are found to be:

$$(4) \quad \sigma_{\text{EW}}(\text{ATLAS}) = 119 \pm 16 \pm 20 \text{ fb} \quad (m_{jj} > 250 \text{ GeV}),$$

$$(5) \quad \sigma_{\text{EW}}(\text{CMS}) = 552 \pm 19 \pm 55 \text{ fb} \quad (m_{jj} > 120 \text{ GeV}).$$

The result from the CMS experiment is twice as precise as the result from the ATLAS experiment. While the use of a smaller dataset causes larger statistical uncertainties in the

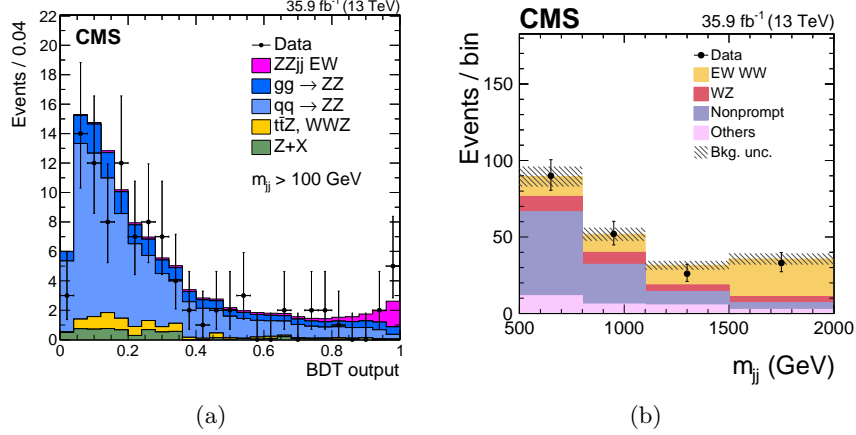


Fig. 4. – (a) Distribution of the output discriminant of a boosted decision tree optimised to extract the signal of electroweak production in $ZZjj$ events. An excess in data is seen and the hypothesis of only strong $ZZjj$ production rejected with a significance of 2.7 standard deviations [22]. (b) Distribution of the dijet invariant mass, m_{jj} , in $W^\pm W^\pm jj$ events. The electroweak production is extracted in a two dimensional fit of m_{jj} and $m_{\ell\ell}$. The background only hypothesis is rejected with a significance of 5.5 standard deviations [23].

measurement by the ATLAS experiment, the larger systematic uncertainties are mainly related to the modelling of the corresponding strong production process. Discrepancies between data and multiple state-of-the-art event generators in the m_{jj} distribution are observed in a kinematic region enriched in the strong production process and correction factors are subsequently derived. The uncertainties related to these correction factors are the largest source of systematic uncertainty in the measurement. The analysis by CMS on the other hand displays a good modelling of the m_{jj} shape. Furthermore, limits on anomalous trilinear gauge couplings are set. They are competitive with limits derived in WW and WZ events.

Studies of vector boson scattering have been performed by the CMS collaboration in $ZZjj$ [22] and $W^\pm W^\pm jj$ events [23] in 35.9 fb^{-1} of pp collisions. The selected sample of $ZZjj$ candidate events consists to 83% of events produced via the strong interaction while only 5% of the events are estimated to originate from the electroweak production. The electroweak signal is extracted in a fit to the output discriminant of a boosted decision tree using seven variables sensitive to the vector-boson-scattering signature as input. The distribution of the output discriminant is shown in Fig. 4(a). The hypothesis of having only the strong production mechanism is rejected with a significance of 2.7 standard deviations where a significance of 1.6 standard deviations is expected. The first measurement of a fiducial cross section of electroweak $ZZjj$ production is in agreement with the theoretical prediction at leading order and found to be:

$$(6) \quad \sigma^{\text{fid.}} = 0.40^{+0.21}_{-0.16}(\text{stat.})^{+0.13}_{-0.09}(\text{syst.}) \text{ fb.}$$

The electroweak $W^\pm W^\pm jj$ production is an ideal probe for vector boson scattering. The production mechanism involves the quartic $WWWW$ vertex. In the scattering of two W bosons with the same electrical charge the corresponding strong production mechanism is highly suppressed and allows for a selection of candidate events with high

purity as shown in Fig. 4(b). To extract the signal the analysis is performed in two-dimensional fits in the dijet and dilepton invariant mass distributions. The event sample is separated into ee , $e\mu$, μe , $\mu\mu$ final states that each have negative or positive charge. The separation into $\ell^+\ell^+$ and $\ell^-\ell^-$ events enhances the sensitivity since the production cross section is asymmetric while the largest source of background is rather symmetric. The background-only hypothesis is rejected with a significance of 5.5 standard deviations where a significance of 5.7 standard deviations is expected. This is the first observation of vector boson scattering and the first observation of a process involving a quartic electroweak vertex. A fiducial cross section of:

$$(7) \quad \sigma^{\text{fid.}} = 3.83 \pm 0.66(\text{stat.}) \pm 0.35(\text{syst.}) \text{ fb}$$

is measured and found in agreement with the leading order theoretical prediction.

Limits on anomalous quartic gauge couplings are set from $ZZjj$ and $W^\pm W^\pm jj$ events and reach an unprecedented stringency. Transverse parameters are constrained to $\mathcal{O}(10^0)/\text{TeV}^4$ and mixed longitudinal and transverse parameters are constrained to $\mathcal{O}(10^1)/\text{TeV}^4$.

5. – Conclusion

The LHC experiments have a rich program of measurements that test the electroweak theory. The most precise of these measurements are performed using single W and Z bosons. Recent measurements of the W boson mass and the effective electroweak mixing angle are approaching a precision competitive with previous measurements at the Tevatron and LEP. However, the systematic uncertainties in these measurements are relatively large and future measurements require an improved theoretical and experimental understanding. Studies of diboson production are entering the precision era with typical uncertainties well below 10%. The stringent constraints on non-Standard Model self interactions are further improved. The large datasets recorded at the LHC render studies on relatively rare electroweak processes possible for the first time. The LHC experiments have studied an increasing amount of processes involving trilinear and quartic interactions. Most notably, the scattering of two W bosons was observed. This is the first observation of vector boson scattering and the first observation of a process involving a quartic electroweak coupling.

REFERENCES

- [1] ATLAS Collaboration, JINST **3** (2008) S08003.
- [2] CMS Collaboration, JINST **3** (2008) S08004.
- [3] LHCb Collaboration, JINST **3** (2008) S08005.
- [4] L. Evans and P. Bryant, JINST **3** (2008) S08001.
- [5] ATLAS Collaboration, Eur. Phys. J. C **78** (2018) no.2, 110.
- [6] S. Catani, L. Cieri, G. Ferrera, D. de Florian and M. Grazzini, Phys. Rev. Lett. **103** (2009) 082001
- [7] ATLAS Collaboration, JHEP **1608** (2016) 159
- [8] R. Corke and T. Sjostrand, JHEP **1103** (2011) 032
- [9] CDF Collaboration, Phys. Rev. Lett. **108** (2012) 151803
- [10] M. Baak *et al.*, Eur. Phys. J. C **74** (2014) 3046
- [11] CMS Collaboration, CMS-PAS-SMP-14-007, <http://cds.cern.ch/record/2139655>

- [12] ATLAS Collaboration, ATL-PHYS-PUB-2017-021, <http://cds.cern.ch/record/2298152>
- [13] CMS Collaboration, CMS-PAS-SMP-16-007, <http://cds.cern.ch/record/2273392>
- [14] ALEPH, DELPHI, L3, OPAL and SLD Collaborations, LEP Electroweak Working Group, SLD Electroweak and SLD Heavy Flavour Group, Phys. Rept. **427** (2006) 257
- [15] CDF and D0 Collaborations, arXiv:1801.06283 [hep-ex].
- [16] LHCb Collaboration, JHEP **1511** (2015) 190.
- [17] ATLAS Collaboration, JHEP **1712** (2017) 059.
- [18] CMS Collaboration, Eur. Phys. J. C **78** (2018) 165
- [19] ATLAS Collaboration, Phys. Rev. D **97** (2018) no.3, 032005.
- [20] ATLAS Collaboration, Phys. Lett. B **775** (2017) 206.
- [21] CMS Collaboration, arXiv:1712.09814 [hep-ex].
- [22] CMS Collaboration, Phys. Lett. B **774** (2017) 682.
- [23] CMS Collaboration, Phys. Rev. Lett. **120** (2018) no.8, 081801.